3D Optimized Reconstruction of a Point-to-Plane Spark Discharge

ANTONIO AMAYA-GARCIA[1], CARLOS AVILÉS-CRUZ[1], JOSÉ LUIS HERNÁNDEZ-ÁVILA[2], RENÉ ARECHIGA-MARTÍNEZ[1]
[1]Departamento de Electrónica, [2]Departamento de Energía
Universidad Autónoma Metropolitana – Azcapotzalco
Av. San Pablo 180, Col. Reynosa, C. P. 02200, Mexico D. F.

ABSTRACT

Abstract: In this paper, a new three-dimensional optimized reconstruction of a spark discharge is proposed. A Discharge process is analyzed in gas atmosphere for two different electrodes. New tools employed to characterize the electrical insulation increase the knowledge about the physical phenomena involved in the development of electrical discharge processes. This work reports the progress of a 3D reconstruction of a spark discharge. The reconstruction is based on a mesh method called Simplex. After simplex mesh reconstruction, a mesh optimization is applied to reduce the number of polygons of the polyhedron, taking into account the gradient across the channel. The 3D optimized reconstruction takes into account the orthogonal projections of images taken by two digital cameras. Such reconstruction is done with a point-plane electrode system, with distance between 3mm and 30 mm. Negative pulse voltage from 40 kV up to 70 kV was applied to the point electrode. Atmospheric air was used as electrical insulator.

Key words: discharges, 3D reconstruction, simplex method.

1 Introduction

One common process for creating a model is the characterization of a phenomenon. In this work, we are making the 3D reconstruction of spark discharges. This reconstruction process is based on the information obtained through digital images of the spark discharges. Previous works about characterization of spark discharges, based on digital images, has been reported following a two dimensional analysis [1][2]. Of particular interest is the characterization of the path of an electrical discharge, since the cause of the spark behavior could be related to the electrical field strength and to the ionized process in the head of the discharge[3][4].

We have developed a reconstruction based on a three dimensional model which has not been done before; or at least, it has never been reported. The reconstruction is based on a mesh method called *Simplex*[5]. After simplex mesh reconstruction, a mesh optimization is applied to reduce the number of polygons of the polyhedron, taking into account the gradient across the channel. 3D optimized reconstruction takes into account two orthogonal projections of images. The images were taken by two digital cameras. The 3D reconstruction phenomena is done with point-plane electrodes array at a distance between 0.3 and 3 cm. Negative pulse voltage from 40 kV up to 70 kV was applied to the point electrode. Atmospheric air was used as electrical insulator

The structure of the paper is organized as follows. Section II gives details of 3D reconstruction process, whereas the polyhedron reconstruction, based on simplex mesh methodology, are given in section III. In order to reduce the number of polygons of the polyhedron, an optimized simplex mesh are detailed in section IV. Whole spark discharge reconstruction is presented in section V and section VI shows results of our proposed approach. Finally, future works and conclusions are presented in section VII.

2 3D Reconstruction Process

The 3D reconstruction process generates a model based on *Simplex* meshes [5]. For this, the digital images of the spark discharges are pre-processed in order to isolate the information of the phenomenon, in order to obtain a 3D model which only represents the spark discharges.

The pre-processing consists of three stages:

1. Filtering.- Using a color-based filter most of the non-phenomenon data in the images is eliminated.
2. Fitting.- Using a region-spreading algorithm, the zone of the images in which the spark discharges appear, is located.
3. Improvement.- With the projection data after the fitting stage, a set of 3D "improved" vertices is created (see ahead), over which the simplex mesh will be created.

The overall process for the 3D reconstruction is shown in Figure 1.

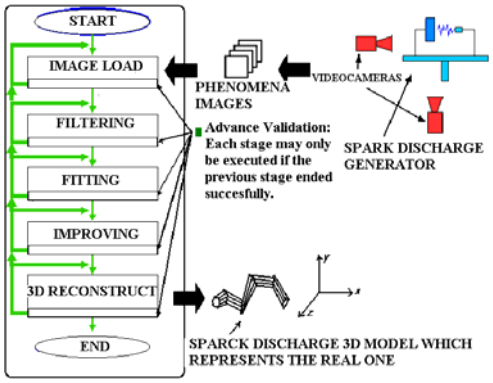

Figure 1: The overall process of the 3D reconstruction of a spark discharge

The images were taken using two video-cameras on independent recording, from which "synchronized" frames were taken.

The synchronization was implemented in two levels: a macro-synchronization based on the video tape timing and a micro-synchronization using an intermittent laser signal, which is visible in the frames.

The video-cameras were positioned in order to obtain orthogonal plane projections. This was implemented by mounting a chassis over the cameras. The chassis includes a laser diode with a beam parallel to the normal vector of the viewing plane of the camera. And using a chassis with a mirror mounted 45 degrees over horizon. The cameras were positioned orthogonally to each other, as shown in Figure 2.

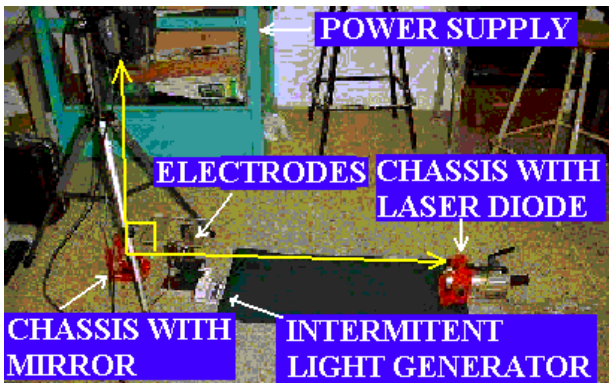

Figure 2: Scheme for image acquisition.

With the acquisition scheme implemented, we developed the pre-processing stages and the 3D reconstruction, described next.

The applied filter is:

$I_f = fc(I)$, where I_f is the image after filtering, and I, the original image. The color filter is defined as:

$$fc(I) = \{p \in I \ IF \ \partial_{R-} \le R(p) \le \partial_{R+} \ AND \ \partial_{G-} \le G(p) \le \partial_{G+} \ AND \ \partial_{B-} \le B(p) \le \partial_{B+}\} \quad (1)$$

Where $R(p), G(p), B(p)$ are the values for the Red, Green and Blue components of the p pixel respectively, and $R(p), G(p), B(p) \in [0,255]$.

p is any pixel in the image and $\partial_{R-}, \partial_{R+}, \partial_{G-}, \partial_{G+}, \partial_{B-}, \partial_{B+}$ are the minimal and maximal thresholds for each color band, and $\partial_{R-} \le \partial_{R+}, \partial_{G-} \le \partial_{G+}, \partial_{B-} \le \partial_{B+}$

For the fitting stage we first look for a pixel that satisfies the next criteria:

$$\begin{aligned} &(\partial_{R-} + \Delta r) \le R(q) \le (\partial_{R+} - \Delta r) \ AND \\ &(\partial_{G-} + \Delta r) \le G(q) \le (\partial_{G+} - \Delta r) \ AND \\ &(\partial_{B-} + \Delta r) \le B(q) \le (\partial_{B+} - \Delta r) \\ &\forall \ \Delta r \in [0,...255] \end{aligned} \quad (2)$$

Where Δr restricts the range of the filter. A pixel that satisfies these criteria is named the "root" pixel and is used to define the image after fitting, as follows: $I_e = En(I_f)$ where

$$\begin{aligned} &En(I_f) = \{p \in I_f \ IF \ there \ is \ a \ path \ of \\ &8\_neighbors \ of \ p \ "root" \ pixel \ AND \\ &\partial_{R-} \le R(t) \le \partial_{R+}, \ \partial_{G-} \le G(t) \le \partial_{G+}, \\ &\partial_{B-} \le B(t) \le \partial_{B+} \ y \ \partial_{R-} \le R(p) \le \partial_{R+}, \\ &\partial_{G-} \le G(p) \le \partial_{G+} \ y \ \partial_{B-} \le B(p) \le \partial_{B+}\} \end{aligned} \quad (3)$$

Where t is an element of the path that is being constructed. It is said that a pixel 'q' is an 8_neighbor of an 'r' pixel if 'q' is adjacent horizontal, vertical or diagonally to 'r'.

Experimentally it was determined that:

$$\begin{aligned} &\partial_{R-} = 52, \partial_{R+} = 255, \partial_{G-} = 6, \partial_{G+} = 170, \\ &\partial_{B-} = 4, \partial_{B+} = 255, \Delta r = 5 \end{aligned} \quad (4)$$

had a good response, but these parameters are variable.

The improvement stage generates a set of 3D vertices, $V_r \in \Re^3$ and is described next:

Define $\Delta x, i$ as the number of horizontal pixels with information of the phenomenon in the image of the frontal view, for *i* pixel column. and $\Delta y, j$ number of vertical pixels with information of the phenomena in the image of the top view, for the *j* column of pixels. As shown in Figure 3.

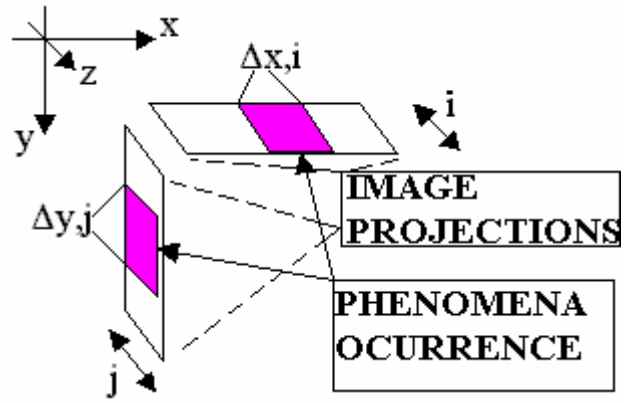

Figure 3: Parameters of the projections

$\Delta x, i$ and $\Delta y, j$ are used to define the minor and mayor radius of the ellipse in whose perimeter are distributed the vertices that define the shape of the 3D model.

Now, let $X(P_{i,j}), Y(P_{i,j}), Z(P_{i,j})$ be the *X*,*Y* and *Z* components of a 3D point $P \in \Re^3$. Then, based on these definitions, we say that the vertices set $V_r \in \Re^3$, that are obtained after the improving stage is given by:

$V_r = V_{hs} \cup V_{hi} \cup V_{li} \cup V_{ld}$, where: (5)

$V_{hs} = \{ v \in \Re^3 \mid$ X(v) is the X coordinate of a non-zero pixel in the top image in column i and Y(v) is the max(all non-zero pixels in the frontal image, in i column), I=[0,1,2 … (length of frontal image)-1]

$V_{hi} = \{ v \in \Re^3 \mid$ X(v) is the X coordinate of a non-zero pixel in the top image in column i and Y(v) is the min(all non-zero pixels in the frontal image, in i column), I=[0,1,2 … (length of frontal image)-1]

$V_{li} = \{ v \in \Re^3 \mid$ Y(v) is the Y coordinate of a non-zero pixel in the frontal image, in column j and X(v) is the max(all non-zero pixels in the top image, in j column), j=[0,1,2, … (length of top image)-1]}

$V_{ld} = \{ v \in \Re^3 \mid$ Y(v) is the Y coordinate of a non-zero pixel in the frontal image, in column j and X(v) is the min(all non-zero pixels in the top image, in j column), j=[0,1,2, … (length of top image)-1]}

With this we have all the pixels that define the shape of the projected volume. But this volume has a rectangular shape, so we also adjust it to an ellipsoidal one, as shown in Figure 4.

If $V_{si} = \{ v \in V_r \mid Z(v) = i \}$, $i = 1,2,3,...,n$, we adjust each element of each V_{si} with:

Let $v_k \in V_{si}$ with k=[0,1,2,...,$|V_{ri}|$ -1], then

X(v_k)=0.5*max(X(v_m)-X(v_n))*sine(k*360), (6)

Y(v_k)=0.5*max(Y(v_m)-(v_n))*cosine(k*360), (7)

$v_m, v_n \in V_{si}$

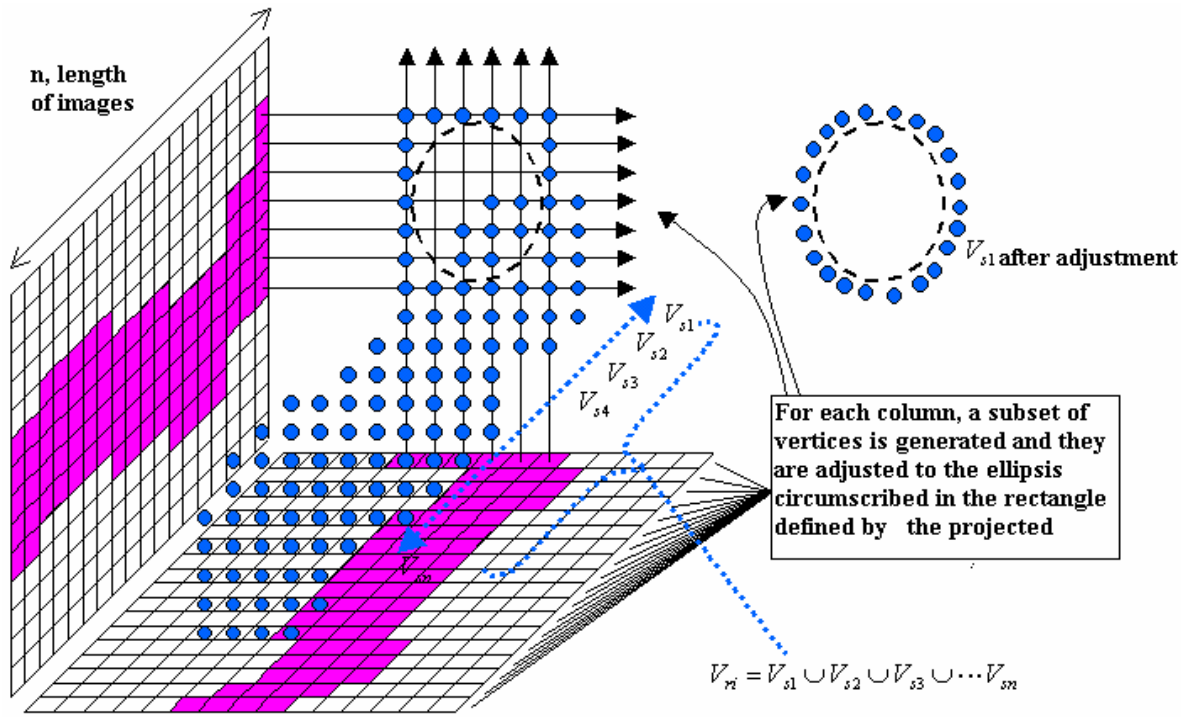

Figure 4: Shape vertices representation.

Leaving $V_{ri} = V_{s1} \cup V_{s2} \cup V_{s3} \cup \cdots V_{sn}$ as the set of vertices that define the shape of the 3D model, but this is not finished yet, because we still have to define the edges that connect the vertices, so that the model is a simplex mesh.

The 3D reconstruction defines edges that connect vertices, following the next rules:

3 Polyhedron Reconstruction

Starting from the top and lateral orthogonal views, the 3D cylindrical polyhedron reconstruction is done; so we have a continuous 2D function (explained in the previous chapter). Now the mesh reconstruction is done. The cylinder can be sampled by n-images (longitudinally) and by m samples per image (see Figures 5 and 6). Then the Mesh reconstruction is applied. We have used simplex mesh methodology at 2-simplex mesh configuration; it means that each polyhedron vertex could be connected with other three vertices, as it can be seen in figure 6.

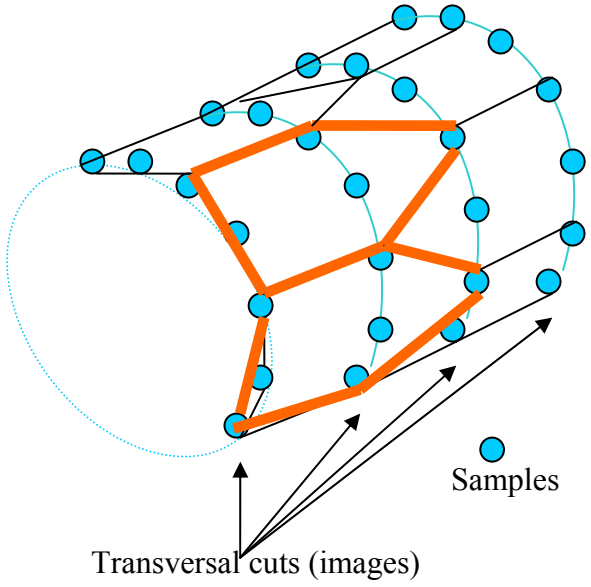

Figure 5: Sampling over cylinder: *n-images* (longitudinally) and *m samples* per image.

Ideally, the number of polygons η is determined as a function of two parameters, the first one is the number of images taken n (transversal cuts number), and the second one is the number of samples m taken per image. The number of polygons η can be estimated by the followings equations:

Case 1) when the number of images is an even number, and the number of samples is even number, for $m \geq 4$, and $n \geq 4$:

$$\eta = \frac{m \cdot n}{4} \tag{8}$$

Case 2) when the number of images is an odd number and the number of samples is an even number, for $m \geq 4$, and $n \geq 3$:

$$\eta = \frac{m \cdot (n-1)}{4} \tag{9}$$

Case 3) when the number of images is an odd number and the number of samples is an odd number, for $m \geq 3$, and $n \geq 5$, we have two cases

i) When the image number (n-1) is divisible by four:

$$\eta = \frac{m \cdot (n-1)}{4} \tag{10}$$

When the image number (n+1) is divisible by four:

$$\eta = \frac{m \cdot (n-1) - 2}{4} \tag{11}$$

Case 4) when the number of images is an even number and the number of samples is an odd number, for $m \geq 3$, and $n \geq 4$, there are two cases:

ii) When the image number n is divisible by four::

$$\eta = \frac{m \cdot n}{4} \tag{12}$$

iii) When the image number (n-2) is divisible by four:

$$\eta = \frac{m \cdot n - 2}{4} \tag{13}$$

As an example, if we take 224 images and 30 samples per image, then the number of polygons created are 1680 (This corresponds to Case 1)

$$\eta = (n*m/4) = (224*30)/4 = 1680 \tag{14}$$

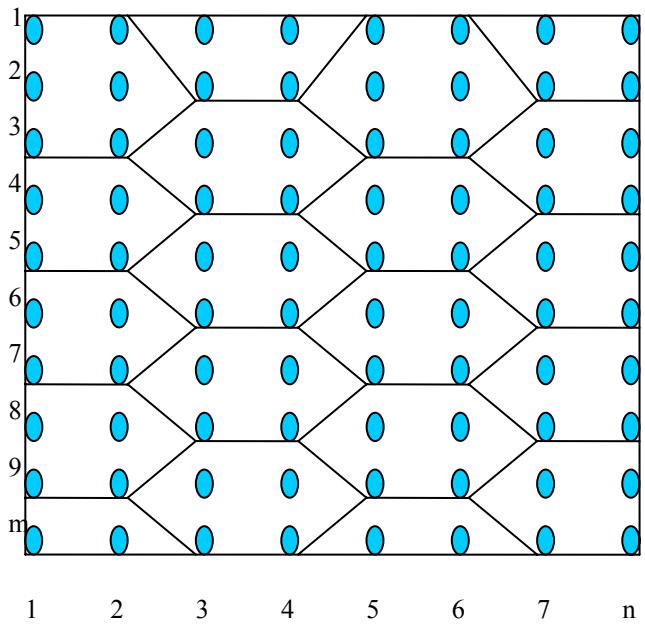

Figure 6: Sampling points over 2D projection: n-images in horizontal axis vs. m-samples per image in vertical axis.

4 Optimized Simplex Mesh

Once the general reconstruction mesh by the simplex method has been obtained, an optimization over it is applied. Optimization is concerned with the localization of the best polygonal distribution units; it is applied across the channel (cylinder) spark reconstruction. Optimization technique is based in local gradient estimation. The next equation represents the gradient for the 2D function (image case), where the norm is taken.

$$|\nabla f(x,y)| = \sqrt{\left(\frac{\partial f(x,y)}{\partial x}\right)^2 + \left(\frac{\partial f(x,y)}{\partial y}\right)^2} \qquad (15)$$

If the gradient is less or equal than a specified threshold, the polygon is eliminated since it is redundant.

5 Spark Discharge Reconstruction

A brief description the electrical experimental set-up it follows: a point-plane electrodes array was employed for the tests. The active electrode is made by a brass rod with a length of 10 cm, finished by a stainless-steel tip point radii of less of 1mm. The earthed electrode is a stainless-steel disk with a diameter length of 12 cm (4 in) and 7 mm width. Both electrodes were aligned horizontally. In order to obtain the negative high voltage pulse, a negative 20 kV DC high-voltage supply (Spellman SL600R) is employed to charge a four capacitor-bank (each capacitor with 3.2 nF @ 30kV maximum of charge) in a Marx array, so it is possible to obtain up to 70 kV_p pulse. A set of measurements were made for spark occurrence at different gap separations, ranging from 3 mm to 30 mm, and negative pulse voltage from 40 kV_p up to 70 kV_p.

The spark discharge characterization was done with help of this ·3D reconstruction tool. Spark voltages (V_s) were taken for each distance at least, three times and the reconstruction of the spark image was done for each sample. Figure 7 shows two examples of the original images used for the 3D reconstruction (for one spark condition). Figure 7(a) shows the horizontal view, parallel to the phenomenon and Figure 7(b) shows the top view, orthogonal to the parallel view.
From these images, the spark discharges are isolated, taking only the blue zone. The images are also synchronized by a laser ray. The Methodology presented in Figure 1, was applied until the 3D reconstruction is accomplished.

All the stages shown in Figure 1 have been implemented with a software tool, which allows to manually define the parameters for the thresholds in the filter and also to define the "root" pixels for the fitting, among other features. With this software the laboratory experiments were done.

6 Results

Once the methodology was defined and the physical phenomenon implemented, we proceeded to process images in order to obtain the cylindrical reconstruction. Two electrodes were used, the first one is aluminum (plane electrode) and the second one is tungsten (point electrode). The main propose of this work is 3D optimized reconstruction of point-plane spark discharge (computationally). The electrical parameters of the physical phenomenon were set up as follows: inter-electrodes distance: 5mm; applied voltage: 30 kV.

Figure 7 shows two images of the phenomenon; Figure 7(a) shows the horizontal view and Figure 7(b) shows the top view. Those images are orthogonal; parallel and orthogonal to the spark discharge, respectively. Starting from these images, the proposed computational methodology was applied: color filtering, images synchronization, fitting and improvement, until 3D reconstruction.

The 3D mesh reconstruction is then ready to be optimized. Figure 8 shows an example with and without optimization. Figure 8(a) presents the 2-simplex mesh [3] reconstruction without optimization. This reconstruction gives a total of 2,780 polygons (220 images, 50 samples per image). Figure 8(b) presents an optimized example at 5 degrees of gradient. This optimized reconstruction gives a total of 1075 polygons.

The algorithm was also tested with different gradient values, from about one to 8 degrees. Table 1 shows results of number of polygons needed for a good reconstruction (220 images, 30 samples per image). We

can see from table 1, that there is a 27% polygon's reduction while varying the gradient from 1 to 8 degrees. No significant degradation occurs when making the reconstruction of the image in the range going from 1 to 5 degrees (see Figures 9(a) and 9(b)).

Other test was also developed on the 3D reconstruction algorithm. Now at 50 samples per image, keeping 220 images. The results are shown in table 2. There is a 27% reduction in the number of polygons when going from 1 to 8 degrees. The same reduction of polygons is obtained, making the reconstruction with 30 and 50 samples per image (see Table 1 vs. Table 2)

7 Conclusions and Future Wworks

A 3D reconstruction of spark discharges employing a mesh method called *Simplex* was presented. From general simplex mesh reconstruction, an optimization was applied based on gradient criteria. The optimized procedure gives 27% reduction in the number of polygons (at 5 degrees of gradient).

With the optimized methodology, there is a reduction in processing time of the spark discharge of about 30%, for the following operations: 3D mesh reconstruction, rendering and visualization time.

Different expressions were developed to find ideal number of polygons for the 2-simplex meshes' method. The number of polygons for mesh reconstruction can be obtained as a function of the number of images and the number of samples per image.

Future work consists in the characterization of spark discharge, and the relation between electrical parameters and the physical phenomenon. Such characterization will make use of statistical features such as fractal dimension and density functions. Finally, a propagation model will be proposed taking into account those statistical features.

REFERENCES

[1] Bañuelos Velázquez E. and Jiménez Rojas R. "*Estudio de la rigidez dieléctrica de una línea de alta tensión en aire sometida a una flama directa y análisis de la trayectoria de la descarga eléctrica*" UAM Azcapotzalco, Energy Dept. 2001 (In Spanish)

[2] Hernández-Ávila J. L., Robledo-Martínez A., Escarela-Pérez R., *"Air Insulation Strength for DC Voltages when Gap is Bridged by Flames*". *Proc. 35th UPEC 2000, paper 207, North Ireland, 2000.*

[3] Watson D. B., Kho S K and Samuels K A , "Impulse flashover of air in divergent fields", J. Phys. D: Appl. Phys. 25 , 1777-1779 (1992).

[4] Alexandrov N. L. Bazelyan E. M., "The Peculiarities of Long-Streamer Propagation in Gases With Strong Electron Attachment", Proc. XIII International Conference on Gas Discharges and Their Applications. Vol. 1, pp 430-433, Glasgow 3-8 September, 2000.

[5] Delingette H.,"*General Object Reconstruction based on Simplex Meshes"*. International Journal of Computer Vision, 32, pp. 111-142, Kluwer Academic Publishers, 1999.

[6] Achat S, Teisseyre Y and Marode E., *"The scaling of the streamer-to-arc transition in positive point to plane gap with pressure*", J. Phys. D.: Appl. Phys., 25, 661-668, 1992.

[7] Aleksandrov N L, Bazelyan E M, Kochetov I V and Dyatko N A, *"The ionization kinetics and electric field in the leader channel in long air gaps"*, J. Phys. D: Appl. Phys. 30 No 11, 1616-1624, 1997.

[8] D. H. Qiu, J. M. K. MacAlpine, "*An Incremental Analysis of Spark Paths in Air Using 3-dimensional Image Processing*", IEEE Transactions on Dielectrics and Electrical Insulation, pp. 758-763, Vol. 7 No. 6, December 2000.

[9] W. E. Lorensen, H. E. Cline, "*Marching Cubes: A High Resolution 3D Surface Construction Algorithm*", Computer Graphics (Proceedings of SIGGRAPH 87), Vol. 21, No. 4, pp. 163-169.

[10] F. Bernardini, J. Mittleman, C. Silva, G. Taubin, H. Rushmeier, "*The Ball-Pivoting Algorithm for Surface Reconstruction"*, IEEE Transactions on Visualization and Computer Graphics, Vol. 5, No. 4, October-December 2000.

[11] W. Niem, M. Steinmetz, "*Camera Viewpoint Control for the Automatic Reconstruction of 3D Objects"*, SPIE Proceedings, Vol. 2182, 1996.

[12] H. Delingette, "*Simplex Meshes: a General Representation for 3D Shape Reconstruction*", Conf. on Computer Vision and Pattern Recognition (CVPR '94).

[13] G. Vogiatzis, P. Torr, R. Cipolla, "*Bayesian Stochastic Mesh Optimisation for 3D Reconstruction*". Conf. on Computer Vision and Pattern Recognition (CVPR '94).

[14] A. Shahrokni, H. Soltanian-Zadeh, R. A. Zoorofi, "*Fast Skeletonization Algorithm for 3-D Elongated Objects"*. Conf. on Computer Vision and Pattern Recognition (CVPR '94).

[15] S. Hasino, "*Three-Dimensional Reconstruction of Fire from Images*", Master Thesis, University of Toronto.

[16] G. Ori and G. Nathan, Gurewich Visual C++ 6 quick start, ebook, release 2003.

[17] [18] Edward Angel, Interactive Computer Graphics: A top-down approach, Addison Wesley, 3rd Edition, 2003.

[18] Akeley K., Segal M., The OpenGL® Graphics System: A Specification Version 2.1, 2006

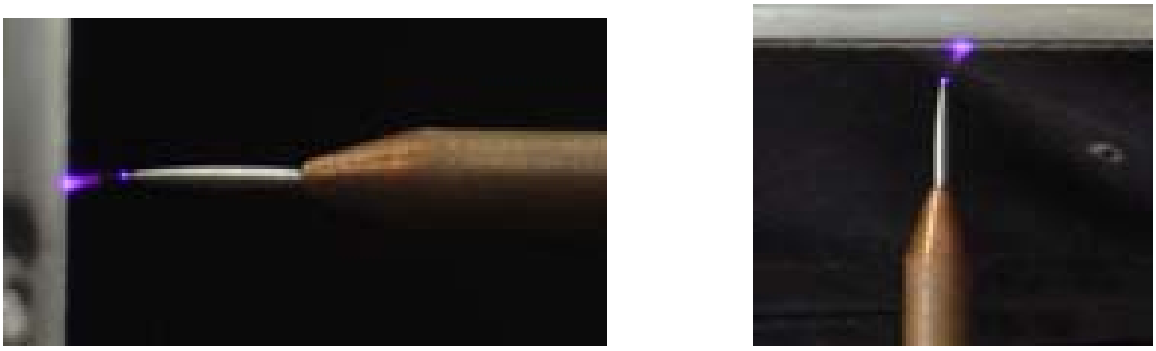

(a) **(b)**

Figure 7: Original images taken from phenomena: a) Horizontal view and (b) upper view

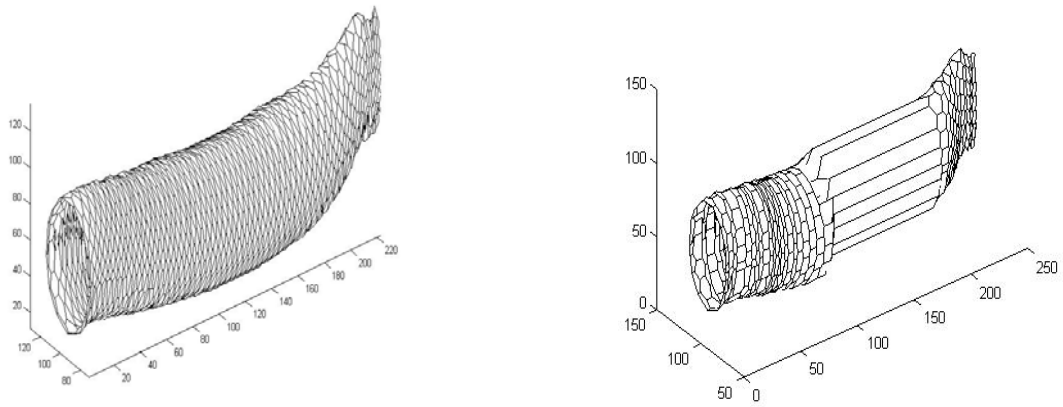

(a) **(b)**

Figure 8: A 3D reconstruction examples (V_s: -30 kV, d: 5 mm.): (a) Without polygonal optimization: 7,700 polygons; (b) With optimization: 1075 polygons at 5 degrees of gradient

Gradient Threshold	Polygons number
±1º - 0.0175 rad.	720
±2º - 0.0349 rad.	705
±3º - 0.0524 rad.	690
±4º - 0.0698 rad.	660
±5º - 0.0893 rad.	645
±6º - 0.1047 rad.	615
±7º - 0.1222 rad.	585
±8º - 0.1396 rad.	525

Table 1: Polygons optimization as a function of gradient threshold (at 220 images and 30 samples per image).

Gradient Threshold	Polygons number
±1º rad.	1200
±2º rad.	1175
±3º rad.	1150
±4º rad.	1100
±5º rad.	1075
±6º rad.	1025
±7º rad.	975
±8º rad.	875

Table 2: Polygons optimization as a function of gradient threshold (at 220 images and 50 samples per image).

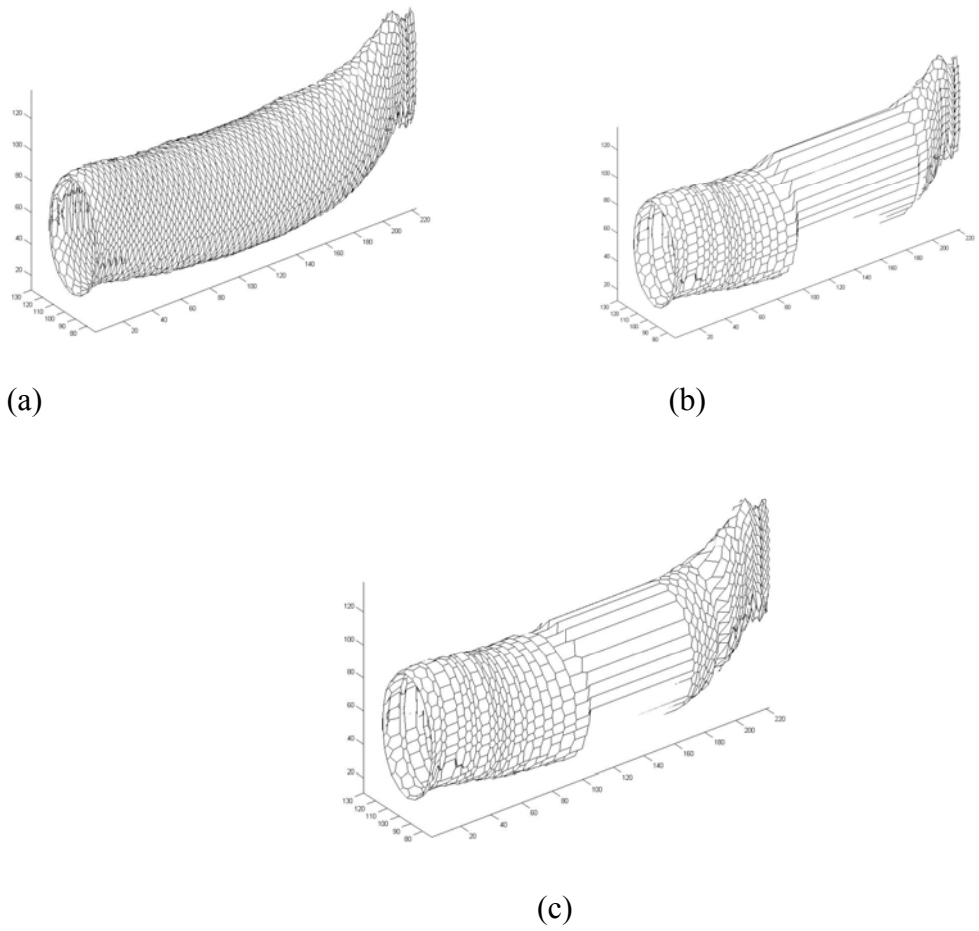

(a) (b)

(c)

Figure 9: 3D Reconstructions as function of gradient and polygons units: (a) Without polygonal optimization: 7,700 polygons (220 images and 140 samples per image); (b) With optimization: 875 polygons at 8 degrees of gradient (220 images and 50 samples per image); (c) With optimization: 1075 polygons and 5 degrees of gradient (220 images and 50 samples per image).